Light trapping in solar cells: Analytical modeling

Mathieu Boccard, Corsin Battaglia, Franz-Josef Haug, Matthieu Despeisse, and Christophe Ballif
Ecole Polytechnique Fédérale de Lausanne (EPFL), Institute of Microengineering (IMT), Photovoltaics and Thin Film Electronics Laboratory, Rue A.-L. Breguet 2, CH-2000 Neuchâtel, Switzerland

(Received 25 July 2012; accepted 26 September 2012; published online 8 October 2012)

We model analytically light harvesting in realistic solar cells by extending a formalism suggested by Deckman *et al.* [Appl. Phys. Lett. **42**, 110968 (1983)], based on tracing of an average ray of light. Arbitrary light scattering schemes and parasitic absorption are implemented in the model, and we validate our approach by comparing with experimental measurements from microcrystalline silicon devices. The intuitive understanding obtained with this extended model is discussed. This approach enables identifying parasitic absorption as main limitation of state-of-the-art light harvesting schemes, and highlights that a better light trapping requires improving the first scattering events. © *2012 American Institute of Physics*. [http://dx.doi.org/10.1063/1.4758295]

Photovoltaic energy is very attractive as it is based on globally abundant, free, and daily renewed sunlight. To meet the worldwide energy demand at a competitive cost, it still has to be improved, either in terms of cost for existing high-efficiency devices or in terms of efficiency for existing cost-effective technologies. A better light harvesting can help in both cases, by allowing either for thickness reduction and material saving or for stronger light absorption and thus higher current output.

Thin-film silicon solar cells rely particularly on light trapping, thus most simulations aiming at better understanding the current limitations of light trapping are applied to this technology. Common approaches include rigorous solving of the Maxwell equations, scalar scattering theory, ray tracing, or waveguide theory.[1–9] Whereas these approaches can provide an accurate prediction of light harvesting, there is often a compromise to find between precision and computer-time consumption. Also, these approaches lack some intuitive understanding of the main phenomena governing light trapping. On the contrary, Deckman *et al.* suggested thirty years ago[10] an analytical equation to intuitively represent light scattering from a random texture, basically by tracing an average ray through the device. This approach naturally leads to the famous $4n^2$ light path enhancement limit in the weak absorbing region,[11] but Deckman assumes a Lambertian distribution of light in the device, which is usually not immediately achieved with experimental light trapping schemes.[12]

We suggest here to extend the formalism of Deckman *et al.* to experimental light trapping schemes, in order to represent light management in real thin film silicon solar devices. To quantify experimental light trapping schemes, we use the recent developments by Dominé *et al.* which allow the direct evaluation of the angular distribution of light transmitted through a rough dielectric–silicon interface, by using only the topology of this surface.[12] Further implementing primary reflection and parasitic absorption (e.g., in doped layers, electrodes, and back reflectors) leads us to analytical expressions giving access to the repartition of light hitting a solar cell between its different destinies; these destinies include the creation of an electron-hole pair ideally to be collected (external quantum efficiency, *EQE*), escape from the cell (reflection, *R*), and parasitic absorption, A_P (representing $100\% - EQE - R$).

In the last part, we validate this extended formula by comparing simulation and experimental measurements (for both *EQE* and *R* curves) for state-of-the-art microcrystalline silicon ($\mu c-\mathrm{Si:H}$) solar cells, and finally we discuss the limitation of our approach and the intuitive understanding that it brings about light management in solar cell.

The light trapping strategy studied here is based on the scattering properties of rough interfaces between the high-index photoactive layer (such as silicon) and the surrounding medium (usually a transparent conducting oxide (TCO)). Scattering elongates the light path in two ways: first, light is forced to cross the thin film slanting, second, if light is scattered at a sufficient angle, total internal reflection can multiply the number of round trips between the front surface and the back reflector. By tracing an average ray of light, as sketched in Fig. 1, Deckman *et al.* derived Eq. (1) giving the absorption probability in the photoactive layer (F^{enh}) in the case of a Lambertian distribution of light in this layer (of thickness, refractive index, and absorption coefficient l, n, and α), and further assuming that this layer is surrounded by a back reflector on one side, and air on the other side.[10]

$$F^{enh} = \sum_{k=0}^{\infty} \underbrace{\left[(1-e^{-2\alpha l}) + e^{-2\alpha l}(1-\eta)(1-e^{-2\alpha l})\right]}_{A_{\text{double pass}}} \cdot \underbrace{\left[e^{-4\alpha l}(1-\eta)(1-1/n^2)\right]^k}_{\text{Attenuation}},$$
$$= \frac{1-\eta e^{-2\alpha l} - (1-\eta)e^{-4\alpha l}}{1-(1-\eta)e^{-4\alpha l} + [(1-\eta)/n^2]e^{-4\alpha l}}. \quad (1)$$

 © 2012 American Institute of Physics

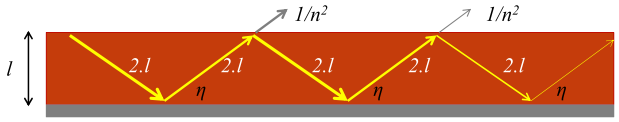

FIG. 1. Cross section of a semiconductor slab between air and a back reflector, with a schematic representation of light trapping by an average Lambertian ray.

Here, F^{enh} is obtained by summing the absorption for each round trip of light in the film ($A_{\text{double pass}}$), while taking into account the losses (Attenuation) between each round trip; these losses are supposed to be parasitic absorptance at the back reflector (η) and escape at the front surface ($1/n^2$). This $1/n^2$ value corresponds to the fraction of light included in the escape cone (defined by the critical angle θ_c) for a Lambertian distribution of light; and the factor two represents the mean light path enhancement for a Lambertian distribution of light.

However, even in state-of-the-art devices, light scattering is not necessarily described by a Lambertian distribution:[12–14] the topology of the rough layer that scatters light is adjusted to enable both light trapping (requiring sharp morphologies) and the growth of a high-quality and homogeneous absorber layer (requiring preferably a smoother surface).[15–17] This compromise usually results in an angular distribution of scattered light which is more pronounced for small angles compared to a Lambertian behavior.[13,18]

To implement an arbitrary angular distribution of light in the formalism developed by Deckman *et al.*, one has to replace the factor two and $1/n^2$ in Eq. (1) by the mean light path enhancement a and the fraction of light included in the escape cone b corresponding to this light distribution. They can be calculated from the angle resolved scattering function $ARS(\theta,\phi)$ with Eqs. (2) and (3), where (θ,ϕ) are the inclination and azimuth of scattered rays of light. $ARS(\theta,\phi)$ can be calculated for the case of scattering from a rough TCO to Si with the method developed by Dominé *et al.*[12,18] using the topology of the TCO surface.

$$a = \int_0^{2\pi}\int_0^{\pi/2} ARS(\theta,\phi)\cdot\frac{1}{\cos(\theta)}\sin(\theta)\cdot d\theta d\phi, \tag{2}$$

$$b = \int_0^{2\pi}\int_0^{\theta_c} ARS(\theta,\phi)\cdot\sin(\theta)\cdot d\theta d\phi. \tag{3}$$

Yet, even though the $ARS(\theta,\phi)$ function for light entering the cell is not Lambertian for experimental devices, Deckman *et al.* already mentioned that "statistical ray optics[11] as well as Monte Carlo simulations have shown that there is an overriding tendency for light initially scattered out of the loss cone to be completely randomized.[19]" This means that the angular distribution of light changes from $ARS_0(\theta,\phi)$ (where the subscript denotes the first scattering event) towards $ARS_{Lamb}(\theta,\phi)=\cos(\theta)/\pi$ while light is traveling back and forth through the device and is scattered at every rough interfaces. We assume thus, as a first order approximation, that the first round trip *only* is driven by the scattering properties of the rough interfaces, and that all light not escaping the device after this first round trip will behave in a Lambertian way, as sketched in Fig. 2. This evolution of the

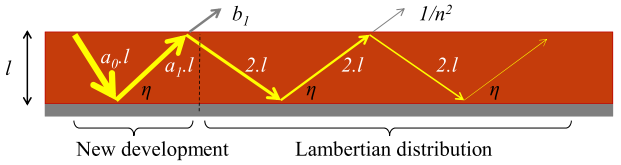

FIG. 2. Cross section of a semiconductor slab between air and a back reflector, with a schematic representation of light trapping by an average ray for a non-Lambertian distribution of light entering the cell.

light distribution will be validated experimentally in the following. Mathematically, this is done by treating separately the first term of the summation with a and b values corresponding to the experimental distribution of light, and setting $a=2$ and $b=1/n^2$ (corresponding to the Lambertian behavior) for the remaining terms:

$$\begin{aligned} F_{ARS}^{enh} = {} & 1-e^{-a_0\alpha l}+(1-\eta)e^{-a_0\alpha l}(1-e^{-a_1\alpha l}) \\ & + e^{-(a_0+a_1)\alpha l}(1-\eta)(1-b_1)\cdot F^{enh}. \end{aligned} \tag{4}$$

Here, a_0 applies to the first pass through the cell, whereas a_1 and b_1 apply to the second pass (i.e., the first way back), as reflection at the back of the device is not necessarily specular. This distinction is particularly important for b_1 which represents the fraction of light included in the escape cone after one round trip, that is thus lost after only 2 passes.

Therefore, our first order approximation requires the calculation of $ARS_1(\theta,\phi)$, corresponding to the first way back. This depends strongly on the light trapping strategy used in the device, and in particular on the back reflector. Metallic reflectors in the close vicinity of silicon and detached back reflectors several microns away from the photoactive layer behave differently.[10,20] Noteworthy, such calculations of $ARS_1(\theta,\phi)$ were recently presented by Bittkau *et al.* for metallic back reflectors.[14]

Then, to complete the modeling of a real device, we further implement primary reflection (R_0) and primary parasitic absorption ($A_P{}^{first}$), occurring for light entering the device, and treat separately parasitic absorption occurring at the front ($A_P{}^{front}$) and at the back ($A_P{}^{back}$) of the cell. The resulting extended formula is given by

$$\begin{aligned} EQE = {} & (1-R_0)(1-A_P{}^{front})\cdot[1-e^{-a_0\alpha l} \\ & + (1-A_P{}^{back})e^{-a_0\alpha l}(1-e^{-a_1\alpha l})] \\ & + e^{-(a_0+a_1)\alpha l}(1-A_P{}^{front})(1-A_P{}^{back})(1-b_1)\cdot F_L^{enh}. \end{aligned} \tag{5}$$

F_L^{enh} corresponds to a Lambertian distribution of light

$$\begin{aligned} F_L^{enh} = {} & (1-R_0)(1-A_P{}^{first}) \\ & \cdot\frac{1-A_P{}^{back}e^{-2\alpha l}-(1-A_P{}^{back})e^{-4\alpha l}}{1-[e^{-4\alpha l}(1-A_P{}^{front})(1-A_P{}^{back})(1-1/n^2)]}. \end{aligned} \tag{6}$$

Similar formulas give access to the amount of light that is parasitically absorbed (at the front and back of the cell), and that is reflected out of the cell.

Here, $A_P{}^{first}$ differs from $A_P{}^{front}$: the former describes the first pass for which light crosses the zone of parasitic

absorption only once, doing so without path enhancement; the latter must account for the eventuality of two passages including path enhancement (in case light is reflected back at the air-glass interface), or no passages if light is reflected directly at the Si-TCO interface.

In the following, we compare simulated and experimentally measured *EQE* and $1-R$ curves for 1 μm to 6 μm thick $\mu c-$Si : H solar cells, deposited on 5 μm thick zinc oxide (ZnO) front electrodes with two different roughnesses, and using a 5 μm thick ZnO back electrode with white paste as back reflector, as described in Ref. 21. The cell configuration is sketched in Fig. 3(a). Both front electrodes scatter all light entering silicon (*Haze* of unity) up to 1100 nm, but with very different $ARS(\theta,\phi)$, resulting in the a_0 and b_0 parameters shown in Fig. 3(b).

In this back reflector configuration, light can be reflected both at the Si-TCO interface and in the white back reflector, making a precise quantification of $ARS_1(\theta,\phi)$ more delicate than with a ZnO/silver back contact as treated in Ref. 14. For a simple estimation of b_1 that lies between b_0 and $1/n^2$, we chose to take the geometrical mean of both, $b_1 = \sqrt{b_0 \cdot 1/n^2}$. This approximation that might appear rough at first sight resulted in a correct representation of the experimental data for many experiments using the presented back reflector configuration. Our model is much less sensitive to a_1 because a_1 mostly impacts the second pass, and not all the following passes as drastically as b_1. We thus arbitrarily set $a_1 = a_0$. This underestimation of a_1 might be thought as a compensation for the probable overestimation of the subsequent a values that are set to 2, whereas in reality the change of the light distribution towards Lambertian is probably more gradual.

We simulated all the experimental data by changing in our model only the thickness of the intrinsic layer (l), or the roughness of the electrode, i.e., a_0, b_1, and R_0. The only input parameter of the equations that was not experimentally obtained, but that was derived from the *EQE*, was R_0, which was set constant for all the spectrum and equal to the R value measured on the cell at 500 nm. Concerning parasitic absorption, whereas $A_P{}^{first}$ was set to the absorptance measured in the absence of light trapping, we found that setting $A_P{}^{front} = 2 \cdot A_P{}^{first}$ was necessary to correctly reproduce experimental data. The same applied to $A_P{}^{back}$, which was set at twice the absorptance value recorded in the absence of light trapping. J_{sc} as a function of thickness is plotted in Fig. 4. A

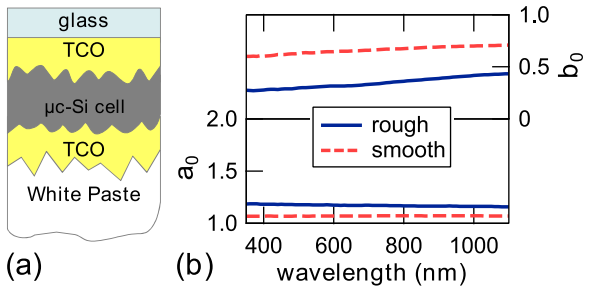

FIG. 3. (a) Schematic view of the device architecture considered here. (b) a_0 and b_0 as a function of wavelength calculated for light scattering in silicon from the rough and smooth electrodes. The scale for a_0 ranges between no light trapping ($a_0 = 1$) and Lambertian light distribution ($a_0 = 2$).

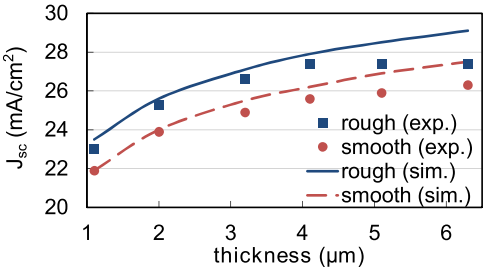

FIG. 4. Current as a function of thickness for $\mu c-$Si : H cells on two differently rough electrodes (experiment and simulation).

good agreement was obtained, except for the discrepancy appearing for large thicknesses (typically after 4 μm) that are mostly due to collection issues in the experimental data, as pointed out in Ref. 21. Importantly, both *EQE* (up to 3 μm thick cells) and R curves are correctly reproduced, as illustrated in Fig. 5 for two thicknesses. The effect of changing the light distribution towards Lambertian after the first scattering event is shown by the dotted curve in Fig. 5. This curve represents the EQE obtained for the 1 μm thick cell on the smooth substrate when using the experimental scattering parameters (a_0, b_1) for all round trips of light. The strong underestimation of the EQE in the 700–900 nm wavelength range validates the evolution of the angular distribution of light towards Lambertian discussed previously.

As a limitation of the model, we should note the absence of the treatment of coherence of light and of near-field effects, and the need for approximation when determining b_1 for detached back reflectors. Practically, near-field effects limit our approach to thicknesses larger than a few λ/n,

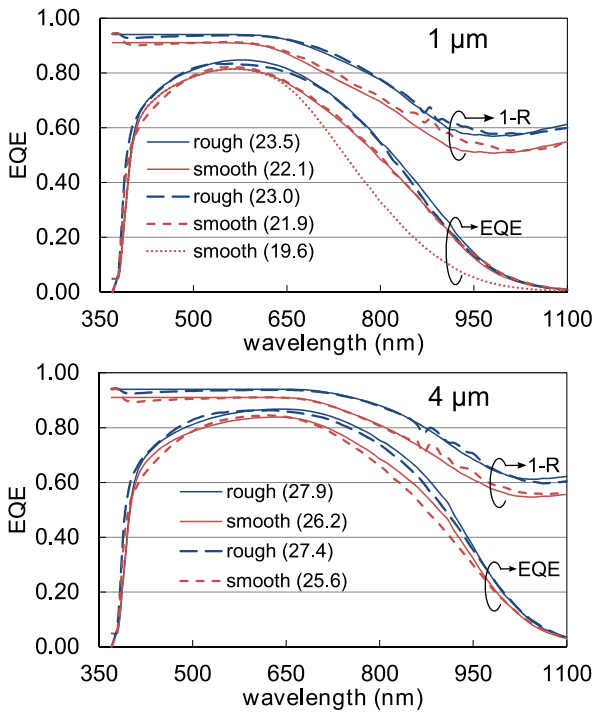

FIG. 5. EQE and $1-$R curves (experiment, dash and simulation, plain) for a $\mu c-$Si : H cell on rough and smooth electrodes, for two different intrinsic layer thicknesses: 1 μm and 4 μm. The numbers in parenthesis are current densities in mA $\cdot$ cm^{-2}. The dotted line is a simulation of the 1 μm thick cell on the smooth substrate using the experimental scattering parameters (a_0, b_1) for all passes.

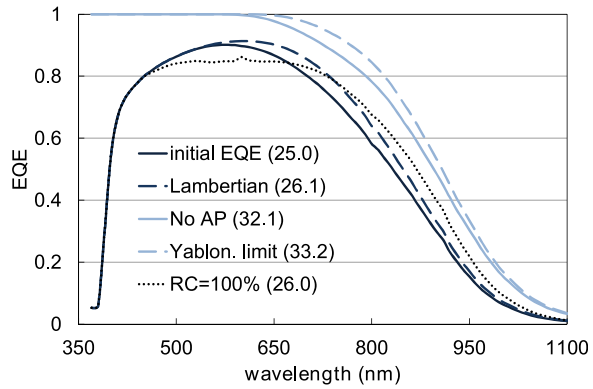

FIG. 6. Simulated EQE curves of a 1 μm thick $\mu c-Si:H$ cell on a rough electrode (initial EQE), and EQE to expect when going to Lambertian light scattering (Lambertian), suppressing all parasitic absorption (No AP), or using an absorber layer of 100% crystallinity (instead of 60% in other cases). The Yablonovitch limit is also indicated. The numbers in parenthesis are current densities in $\text{mA} \cdot \text{cm}^{-2}$. R_0 was set to zero for all curves.

typically over 1 μm for silicon.[11] Also, the abrupt change of light distribution towards Lambertian might lead to an overestimation of the EQE in the wavelength range where the second round trip of light contributes greatly (typically around 700 nm). However, the fairly good agreement with experimental data do not pledge for looking for a more realistic—but more complicated—smoother evolution.

The main objective of our approach was to obtain an intuitive description of the key parameters governing light harvesting in solar cells. These parameters are mainly the absorption in the photoactive layer ($\alpha \cdot l$), light scattering (a_0, a_1, and b_1), and parasitic absorption. We could already point out the impact of the back reflector on light scattering, even in the superstrate configuration (as experimentally observed by Sai *et al.*[22]). To further illustrate the possibility offered by our model, we reproduce in Fig. 6 the *EQE* curves that are potentially obtainable when improving the absorption coefficient (going to 100% of crystallinity), light trapping (going to immediate Lambertian distribution), and parasitic absorption (suppressing it). This is applied to the 1 μm cell on the rough substrate, with primary reflection (R_0) set to zero for all cases. We compare the resulting EQE curves to the one corresponding to the Yablonovitch limit (no parasitic absorption and immediate Lambertian light scattering, corresponding to setting $\eta = 0$ in Eq. (1)), which gives a maximal current of 33.2 $\text{mA} \cdot \text{cm}^{-2}$. Our optical system has the potential to reach 32.1 $\text{mA} \cdot \text{cm}^{-2}$ for no parasitic absorption, indicating that its light trapping capacities are quite close to the Yablonovitch limit. A much lower improvement is obtained when changing other parameters. To go above this limit would require the first scattering events (typically a_1 and b_1) to be improved.

In conclusion, we generalized the formula proposed by Deckman *et al.* to obtain a representation of light management in real solar cells. We suggested an extension of the formula to experimental distributions of scattered light for light entering the cell, by modifying only the first two passes and treating light that do not escape the cell in a Lambertian way. Further implementing primary reflection and parasitic absorption at the front interface of the cell gave rise to a correct reproduction of *EQE* and *R* curves for various microcrystalline silicon solar cells. This simple model enables an intuitive representation of light scattering in solar cells, and a fast way of determining the predominant parameters limiting their current output. The most limiting parameter in state-of-the-art devices was shown to be parasitic absorption rather than sub-optimal light trapping, and the particularly important role of scattering light at large angle for the first scattering events was highlighted.

The authors gratefully acknowledge support by the Swiss Federal Energy Office. Part of this work was also funded by the Velux Stiftung and by the EC under Grant agreement No. 283501EU, for the EU FP7 project "Fast Track."

[1]M. Zeman and J. Krc, J. Mater. Res. **23**, 889–898 (2008).
[2]J. Krc, F. Smole, and M. Topic, Prog. Photovoltaics **11**, 15–26 (2003).
[3]A. Naqavi, K. Söderström, F.-J. Haug, V. Paeder, T. Scharf, H. P. Herzig, and C. Ballif, Opt. Express **19**, 128–140 (2011).
[4]C. Rockstuhl, S. Fahr, F. Lederer, F. J. Haug, T. Soederstroem, S. Nicolay, M. Despeisse, and C. Ballif, Appl. Phys. Lett. **98**, 051102 (2011).
[5]T. Lanz, B. Ruhstaller, C. Battaglia, and C. Ballif, J. Appl. Phys. **110**, 033111 (2011).
[6]K. Jäger, M. Fischer, R. A. C. M. M. van Swaaij, and M. Zeman, J. Appl. Phys. **111**, 083108 (2012).
[7]M. Schulte, K. Bittkau, B. E. Pieters, S. Jorke, H. Stiebig, J. Hüpkes, and U. Rau, Prog. Photovoltaics **19**, 724–732 (2011).
[8]Z. Yu, A. Raman, and S. Fan, Proc. Natl. Acad. Sci. U.S.A. **107**(41), 17491–17496 (2010).
[9]D. M. Callahan, J. N. Munday, and H. A. Atwater, Nano Lett. **12**, 214–218 (2012).
[10]H. W. Deckman, C. R. Wronski, H. Witzke, and E. Yablonovitch, Appl. Phys. Lett. **42**, 968 (1983).
[11]E. Yablonovitch, J. Opt. Soc. Am. **72**, 899 (1982).
[12]D. Domine, F.-J. Haug, C. Battaglia, and C. Ballif, J. Appl. Phys. **107**, 044504 (2010).
[13]C. Battaglia, M. Boccard, F.-J. Haug, and C. Ballif, "Light trapping in solar cells: When does a Lambertian scatterer scatter Lambertianly?" J. Appl. Phys. (submitted).
[14]K. Bittkau, W. Böttler, M. Ermes, V. Smirnov, and F. Finger, J. Appl. Phys. **111**, 083101 (2012).
[15]M. Boccard, T. Soderstrom, P. Cuony, C. Battaglia, S. Hanni, S. Nicolay, L. Ding, M. Benkhaira, G. Bugnon, A. Billet, M. Charriere, F. Meillaud, M. Despeisse, and C. Ballif, IEEE J. Photovoltaics **2**, 1–7 (2012).
[16]C. Battaglia, C.-M. Hsu, K. Söderström, J. Escarré, F.-J. Haug, M. Charrière, M. Boccard, M. Despeisse, D. T. L. Alexander, M. Cantoni, Y. Cui, and C. Ballif, ACS Nano **6**, 2790 (2012).
[17]H. Sai, Y. Kanamori, and M. Kondo, Appl. Phys. Lett. **98**, 113502 (2011).
[18]D. Dominé, "The role of front electrodes and intermediate reflectors in the optoelectronic properties of high-efficiency micromorph solar cells," Ph.D. dissertation (University of Neuchatel, 2009).
[19]H. W. Deckman, C. R. Wronski, and H. Witzke, J. Vac. Sci. Technol. A **1**, 578–582 (1983).
[20]E. Moulin, U. W. Paetzold, K. Bittkau, M. Ermes, L. Ding, L. Fanni, S. Nicolay, J. Kirchhoff, A. Bauer, A. Lambertz, C. Ballif, and R. Carius, "Thin-film silicon solar cells with optically decoupled back reflectors," Mater. Sci. Eng. (to be published).
[21]M. Boccard, P. Cuony, M. Despeisse, D. Dominé, A. Feltrin, N. Wyrsch, and C. Ballif, Sol. Energy Mater. Sol. Cells **95**, 195–198 (2011).
[22]H. Sai, H. Jia, and M. Kondo, J. Appl. Phys. **108**, 044505 (2010).